Enhancing the Electrical and Optoelectronic Performance of Nanobelt Devices by Molecular Surface Functionalization

Changshi Lao, Yi Li, C. P. Wong,* and Z. L. Wang*

School of Materials Science and Engineering, Georgia Institute of Technology, Atlanta, Georgia 30332-0245

ABSTRACT

By functionalizing the surfaces of ZnO nanobelts (NBs) with a thin self-assembled molecular layer, the electrical and optoelectronic performances of a single NB-based device are drastically improved. For a single NB-based device, due to energy band tuning and surface modification, the conductance was enhanced by 6 orders of magnitude upon functionalization; a coating molecule layer has changed a Schottky contact into an Ohmic contact without sophisticated deposition of multilayered metals. A functionalized NB showed negative differential resistance and exhibited huge improved photoconductivity and gas sensing response. The functionalized molecular layer also greatly reduced the etching rate of the ZnO NBs by buffer solution, largely extending their life time for biomedical applications. Our study demonstrates a new approach for improving the physical properties of oxide NBs and nanowires for device applications.

Nanowires (NWs) and nanobelts (NBs) have been demonstrated as the fundamental building blocks for fabricating various nanodevices such as FET,[1] gas sensor,[2] diodes,[3] LED,[4] biosensors,[5-8] and others. To improve the performance and further realize the application of nanoscale devices, a few issues need to be addressed such as improving the contacts, increasing the carrier mobility, minimizing the density of surface defects, and improving the device stability. The contact between NBs and metal electrodes is an important part of the entire device.[9] The energy difference between the work function of the metal electrode and the electron affinity of the semiconductor NB forms an energy barrier (Schottky barrier), which hinders the carrier transport in the device. The traditional method for establishing a good contact is a multilayer metal deposition, which increases the complexity of the fabrication. The low concentration of the carrier due to surface defects in the NB is also another factor of deteriorating the device performance.[10] The small size of the NB makes the device highly sensitive to the surface adsorbed molecules, thus the stability of the device is a concern due to high density of surface defects.

The self-assembled thin molecular layer has demonstrated the effectiveness in modifying surface physics and properties of metal and metal oxide materials.[11-13] It acts as a functional group in different nanowire-based devices for chemical and biological sensing.[14-16] In this paper, we have explored a novel approach of using self-assembled thin molecular layer on a surface for improving the electrical and optoelectronic performances of NWs and NBs. A few kinds of molecules were tested and their performances were compared. With the molecular-coated ZnO NBs, the contact properties and the carrier mobility were greatly enhanced. More importantly, the optical and gas sensing performance of these small organic molecule-functionalized ZnO were also greatly enhanced. This process has demonstrated an easy and effective method for improving the performance of the NW/NB-based devices.

Among all of the semiconducting NBs, ZnO is one of the most widely studied materials due to its promising optical, optoelectronic, and piezoelectric properties.[17,18] Furthermore, ZnO has been demonstrated to possess a diversity of novel nanostructures such as NWs, NBs,[19] nanohelices,[20] and nanocombs.[21] ZnO NBs are also the most attractive candidates for applications in field-effect transistor (FET), sensor, and optoelectronics.[22] Our study has been focused on ZnO NBs synthesized by a vapor–solid process.[19]

Various types of carboxylic acid self-assembled molecules with different terminal groups (such as stearic acid, lysine, dodecanedioic acid, mercapto-acetic acid, and perfluorotetradecanoic acid) were used to treat the ZnO NBs. The chemical structures of the acids are shown in Figure 1a. The functionalization was achieved by grafting the −COOH

* Corresponding authors. E-mail: zhong.wang@mse.gatech.edu (Z.L.W.); cp.wong@mse.gatech.edu (C.P.W.).
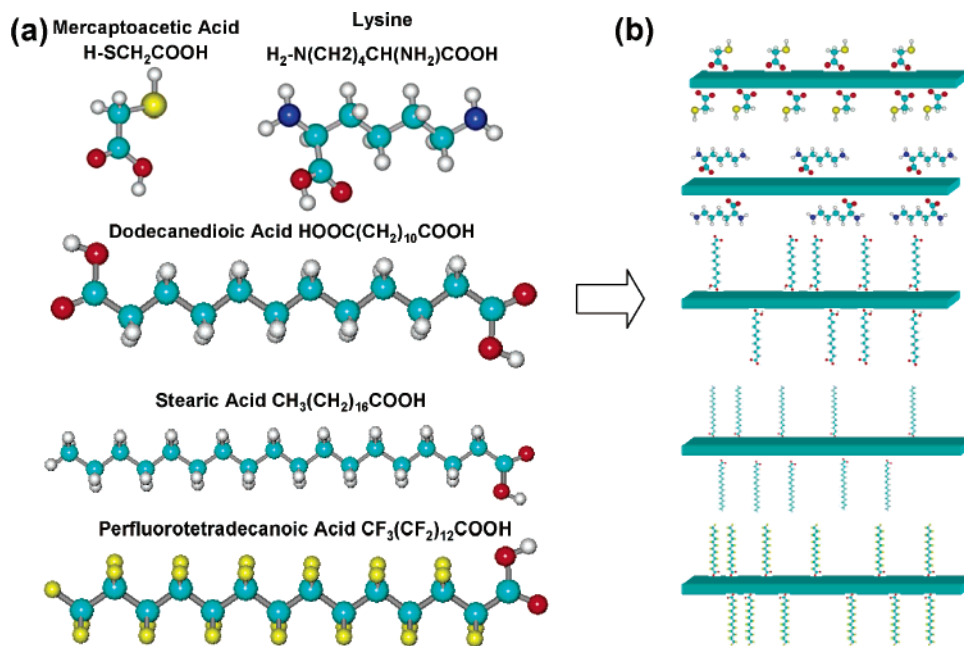
Figure 1. (a) Molecular structures of the five molecules used for surface functionalization. (b) Schematic models of the molecule-functionalized ZnO NBs.

Table 1. Contact Angles of ZnO NBs Film after Acid Treatment

samples	average contact angle, deg
stearic acid	112
lysine	56
dodecanedioic acid	58
mercapto-acetic acid	52
perfluorotetradecanoic acid	115

group onto the surface of ZnO, and the surface properties of ZnO were tailored with different functional groups. The molecular solutions were prepared by dissolving the acids into an ethanol solution with a concentration of 5 mM. Then a small piece of ZnO NB samples was immersed into the solution. After treating the samples at room temperature for 24 h, the ZnO NBs samples were removed from the solution and rinsed with ethanol in order to remove excess unreacted molecules. After drying the ZnO NBs, the contact angle of a deionized (DI) water droplet on a film made of NBs was measured by a goniometer (Rame-Hart Co.). Table 1 shows the results of the contact angle measurement of the treated samples. As can be seen from the table, lysine, dodecanedioic acid, and mercapto-acetic acid-treated substrates showed low contact angles (more hydrophilic), while stearic acid and perfluorotetradecanoic acid-treated surfaces showed high contact angles (more hydrophobic). The difference indicates the successful coating of the thin layers of molecules on ZnO NBs, as shown in Figure 1b. For lysine, dodecanedioic acid, mercapto-acetic acid, the hydrophilic terminal groups ($-NH_2$, $-COOH$, and $-SH$) contributed to the reduced contact angles. On the other hand, stearic acid and perfluorotetradecanoic acid possess hydrophobic terminal groups ($-CH_3$, $-F$), which lead to the high contact angle. These molecule-modified ZnO substrates changed their surface energies and

physical properties that could have a profound influence in their sensing properties.

Increased Electric Conductivity. Single NB-based transport measurement was carried out using the functionalized NB by a special handling process to eliminate surface contamination and/or damage to the passivation layer. The electrode pattern was designed to have a few parallel electrodes separated by 5−20 μm. The molecular-functionalized ZnO NBs were transferred onto the prefabricated electrodes by touching the NB sample with the electrodes. We can easily make a sample with only a single ZnO NB lying across two electrodes by this process. The as-fabricated devices showed very good electric transport performance, as shown in Figure 2a. The black curve is the $I-V$ characteristics of a ZnO NB functionalized with a monolayer of $HOOC(CH_2)_{10}COOH$ (dodecanedioic acid). The green curve is the $I-V$ characteristics of an untreated NB, which is magnified by a factor of 5×10^5 to bring it to the same scale for comparison purposes. Figure 2b shows the conductivity measured for NBs coated with different end-group molecules. In our experiments, 30 samples for each group of devices were tested. More than 90% of the functionalized NB-based devices were conducting, and all of the untreated NB-based samples showed poor conductivity. The NB samples used for the device fabrication were taken from the same type of sample with a dry and clean surface so that the results can be directly compared with each other; the only difference is the layer of molecules functionalized on the surface. As shown in Figure 2a, the current flowing through the molecular-coated NB is around 10^6 times larger than the untreated NB. Figure 2b shows the conductivity for NBs coated with different end-group molecules, indicating a large difference for different molecular-treated ZnO surfaces.
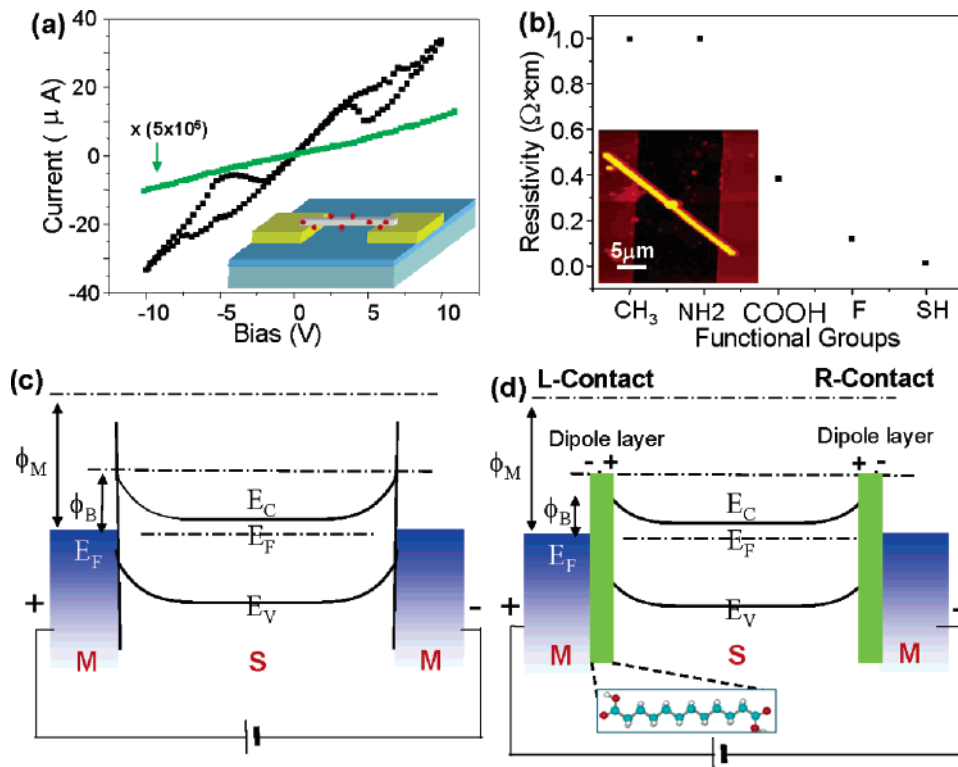
Figure 2. (a) $I{-}V$ characteristics of a ZnO NB functionalized with the self-assembled thin molecule layer, $HOOC(CH_2)_{10}COOH$ (black line), and an untreated ZnO NB sample (green line). The current of the untreated NB is magnified by 5×10^5 times for comparison purpose. Note: no Pt was deposited at the contacts so that the measured current for the untreated NB is low. Inset is a schematic view of the nanobelt device. (b) Resistivity of the NBs coated with different molecules. The lower inset image is an AFM image of a coated NB lying across two electrodes. (c) Energy-level diagram of metal/semiconductor/metal interfaces, ϕ_M is the work function of the metal. There is an energy barrier ϕ_B between the metal contact and the untreated NB. (d) Energy-level diagram of Au electrode and a ZnO NB with a thin molecular layer between. The molecules form an interface dipole layer, which helps to decrease the energy barrier between the NB and Au.

The increased conductivity may be explained from the band structure at the contacts. Figure 2c shows the band structure of the NB at the left-hand-contact (L-contact) and right-hand-contact (R-contact) along a single NB without the coating of a molecular layer at the surface. The contact between Au and ZnO is a Schottky contact of height Φ_B. When a monolayer molecules are introduced at the interface, as shown in Figure 2d, it effectively reduces the barrier height due to the introduction of molecular states between the band gap. The molecular layer may form a dipole at the interface.[23] When a positive voltage is applied from the left- to the right-hand side, the L-contact is a metal−semiconductor (M−S) contact and it is a forward biased Schottky, thus its resistance is very low. At the R-contact, although the S−M contact is a reversely biased Schottky barrier, the dipole layer not only reduces the barrier height but also mediates the transport of electrons (for n-type semiconductor such as ZnO) from the metal contact to semiconductor, which effectively reduces the contact resistance, resulting in a drastic increase in conductance. In fact, a good contact was very easy to establish for the molecular-coated ZnO NB, so the conductivity is very high for the treated NBs.

As shown in Figure 2b, the resistivity of the functionalized NBs with different molecules ranges from 0.1 to 1 Ω-cm for the contacts made simply through a dry transfer, which is 1 order of magnitude lower than that of the as-synthesized

ZnO NBs, which were made in Ohmic contact with the electrodes through several layers of metal deposition using e-beam lithography.[24,25] The great enhancement in conductivity is attributed to the coating molecular layer that forms a highly ordered two-dimensional passivation layer on the surface of ZnO NB, which prevents the oxygen in atmosphere from combining with the point vacancies at the surface. In fact, a combination of a vacancy with an oxygen reduces the carrier density in the NB, thus, lowering the conductivity. Also, after bonding with ZnO NB, the reaction group, carboxyl −COOH changed to −COO⁻, which is an electron donor and can provide an electron to the NB, consequently increasing the carrier density, e.g., the conductivity.

For the $I{-}V$ characteristics of the ZnO NBs functionalized with different end-group molecules, negative differential resistance (NDR) was observed, as shown in Figure 3. Eighty percent of the molecule-coated NBs, regardless of the type of the end-groups, displayed a NDR behavior. The peak to valley ratios in the positive bias $I{-}V$ curves at room temperature ranged from 1.56 (dicarboxylic acids, $HOOC(CH_2)_{10}COOH$, green line) to 1.08 (lysine, $H_2N(CH_2)_4CH(NH_2)COOH$, red line). In the literature, several models have been proposed to explain the origin of the NSR.[26,27] From a previous study on the mechanism of the NDR[28] in molecular carrier transport, the high current peak is associated with
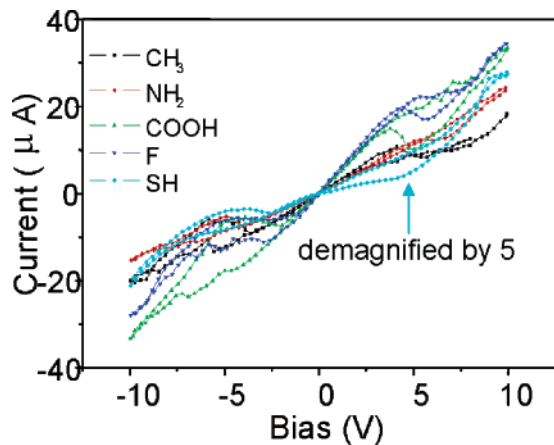
Figure 3. Typical $I-V$ characteristics of the molecular-functionalized ZnO NBs with different end-group molecules, which shows a typical negative differential resistance effect at room temperature. The current for the NB with molecule functionalization layer, $HOOC(CH_2)_{10}COOH$ (blue line), was demagnified by 5 times for comparison purpose.
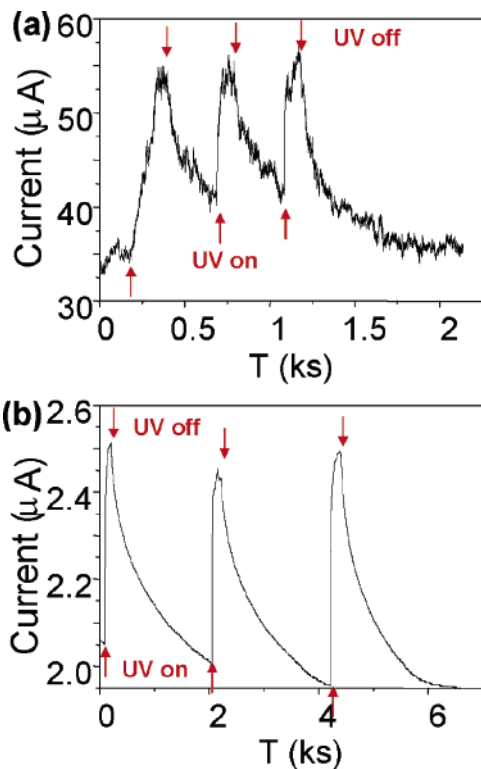
Figure 4. Photocurrent of (a) $HOOC(CH_2)_{10}COOH$-functionalized ZnO NB and (b) untreated ZnO NB when subject to UV light illumination, received under identical measurement conditions. Note: Pt was deposited at the contacts to reduce the contact resistance.

the delocalization of the lowest unoccupied molecular orbital. Under the bias at around 4 V, the charge distribution in coating molecules was disturbed due to a voltage-induced redox reaction. We suspect that the carrier transport of our molecular-functionalized ZnO NBs were also affected by the electronic delocalization. At the bias of 4 V, the bias voltage induced a voltage-induced redox reaction, thus the unoccupied molecular orbital in the coating molecules acted as a
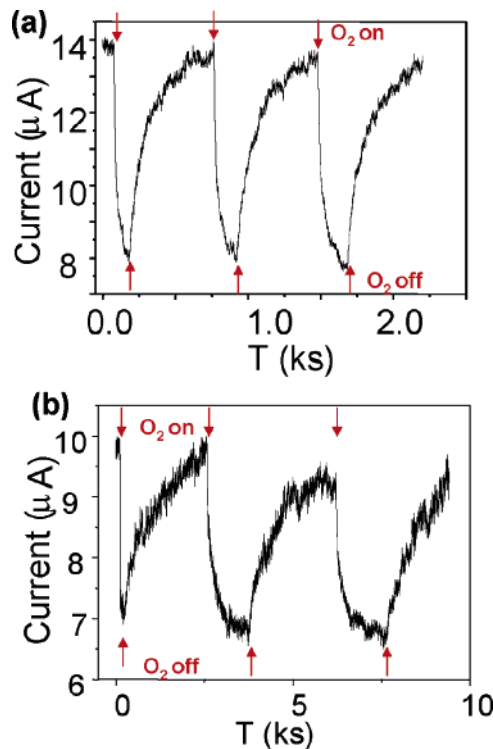
Figure 5. Gas sensing properties of (a) $HOOC(CH_2)_{10}COOH$-functionalized ZnO NB and (b) untreated ZnO NB in responding to O_2 of 154 ppm in concentration. Note: Pt was deposited at the contacts to reduce the contact resistance.

transition state to facilitate the electron−hole excitation in the ZnO NB, possibly resulting in the NDR effect.

Enhanced Photoconductivity. To further test the performance of these functionalized ZnO NB samples and explore their potential applications, we compared the current response under UV light exposuree for a $(HOOC(CH_2)_{10}COOH)$-coated ZnO NB and an untreated NB. The contacts for the untreated ZnO NB and Au electrodes were deposited with Pt by a Focus Ion beam system.[29] The purpose of this process is to eliminate the huge contact resistance of untreated ZnO NB and Au electrodes and get an intrinsic photoresponse of untreated NB. Note that the NBs used for Figure 2 were not deposited with Pt so that the native NB (green curve) has a much lower current. The UV light source used in the experiment is a high-intensity UV lamp with a wavelength of 365 nm. The light intensity at the sample surface was 8900 mW/cm^2. Both the molecular-coated NB and the untreated NB showed an on/off state corresponding to the exposure of the UV light, as shown in Figure 4. Figure 4a is the UV response of the molecular-functionalized NB. The current flowing through the molecule-coated NB increased from 35 to 55 μA upon the exposure of the UV light, a 57.1% enhancement. For the untreated ZnO NB, the current increased from 2.06 to 2.51 μA, a 22% enhancement. The photoresponse of the ZnO NBs to the UV light was enhanced by around 3 times after the functionalization of the ZnO NBs by a coating layer of $HOOC(CH_2)_{10}COOH$, which is an effective and feasible way of enhancing the optical response of NBs for UV detection. The absorption spectrum of a typical organic molecule, which has a similar structure to
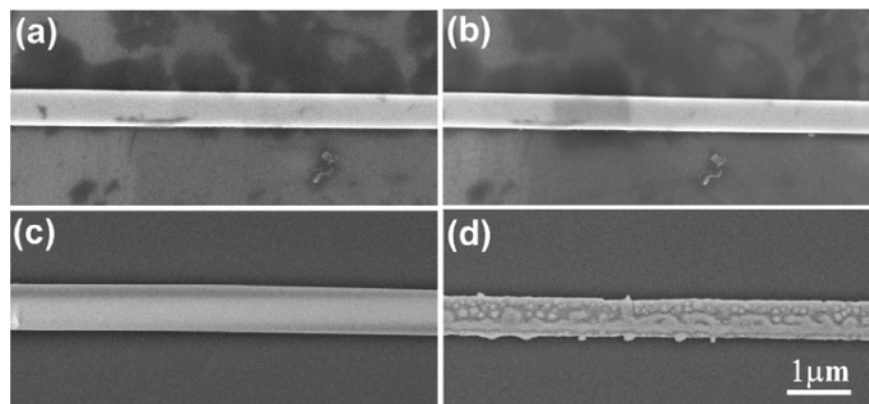
Figure 6. SEM images of the same NB coated with HOOC(CH$_2$)$_{10}$COOH (a) before and (b) after immersing into the buffer solution for 15 min. SEM images of an untreated NB (c) before and (d) after immersing into the buffer solution for 15 min.

that of the molecules used in our experiment, has a strong peak at the wavelength of around 380−400 nm. This means that electrons in the molecules coating were excited to a higher energy state under the exposure of UV light, which left an unoccupied molecular orbital at an energy level that falls within the band gap of ZnO. At the same time, the carriers inside the ZnO NB was also excited under the exposure of the UV light.[10] The unoccupied molecular orbital acted as a transition state for the electron in the valance band of ZnO to transit to the conduction band of ZnO, resulting in a higher efficiency of separating the electron−hole pair and the increased photocurrent efficiency.

High Gas Sensitivity. The coating molecule also enhances the sensitivity of the NB for gas sensors. For oxygen gas with a concentration of 154 ppm, the responses of the treated and untreated ZnO NBs are shown in Figure 5. When the oxygen gas was turned on, the current flowing through the HOOC(CH$_2$)$_{10}$COOH-coated NB decreased from 14 to 8 μA, which is a 43% drop (Figure 5a). For the untreated ZnO NB, the electrode was deposited with Pt on the contacts for reducing the contact resistance and enhancing gas sensing by the NB. The current flowing through the device decreased from 9.7 to 7.0 μA, a 28% drop (Figure 5b). It is apparent that the gas sensing response of the ZnO NBs were enhanced by the functionalization of the HOOC(CH$_2$)$_{10}$COOH. The working temperature of the gas sensor in our experiment was 300 °C. At this temperature, the molecules had been debonded from ZnO NB and partially/fully decomposed. Because of bonding reaction of the carboxyl −COOH group with the ZnO NBs during the functionalization process, there are extra oxygen vacancies being created at the surface of ZnO NBs by functionalization. As such, more oxygen gas can combine with these surface defects after debonding the molecules, the conductance change in the treated NB is more significant compared to that of the untreated NB. This is probably why the treated ZnO NB has higher sensitivity.

Increased Biostability. Our previous study has shown that ZnO nanowires are soluble in biofluids.[30] The biodegradability is very beneficial for some applications. For nanodevices, we wish to increase the life time and biostability of the material so that it can achieve some designed purposes. In this section, we demonstrate that the coating molecules

can protect the ZnO NBs in the buffer solution to substantially extend its lifetime. To test the solubility of the molecular-coated ZnO NBs and the uncoated ZnO NBs, a buffer solution with PH 7.0 (Fisher Scientific SB107-500) was used as the testing reagent. By dispersing the NBs in the solution for a fixed time, then we examine the "etching" result of the surface through SEM. Figure 6a is an SEM image of a HOOC(CH$_2$)$_{10}$COOH-coated NB before immersing into the buffer solution. Figure 6b is a SEM image of the same ZnO NB after 15 min etching in the buffer solution. The NB retained the same morphology before and after the buffer solution treatment. Parts c and d of Figure 6 are the SEM images of an untreated ZnO NB before and after the buffer solution treatment for 15 min. As can be seen in the images, the untreated NB was greatly etched by the buffer solution. The resistance to surface etching might come from the dense and well aligned molecules protecting the surface of ZnO NBs. With the coating of molecules on the surface, the surface chemical and physical properties were changed according to the contact angle measurement. This experiment shows a possible way to increase the stability of ZnO NBs in a biosolution.

In conclusion, we have demonstrated that, by functionalizing the surfaces of a nanobelt/nanowire with a self-assembled thin molecular layer, their electrical and optoelectronic performances are greatly enhanced. The coating molecular layer has effectively decreased the contact resistance between a NB and the Au electrode, resulting in a change of a Schottky contact into an Ohmic contact. Furthermore, the photoconductivity and gas-sensing response of the NBs have been dramatically increased. Last, the functionalized molecules greatly reduces the dissolution rate of ZnO NBs in biofluid; as such, it effectively extends the NW devices life time for biomedical applications. Our study on the molecular-functionalized NWs presents a simple and cost-effective method for improving the performance of oxide nanowire/nanobelt-based devices.

References

(1) Arnold, M. S.; Avouris, P.; Pan, Z. W.; Wang, Z. L. *J. Phys. Chem. B* **2003**, *107*, 659.

(2) Wan, Q.; Li, Q. H.; Chen, Y. J.; Wang, T. H.; He, X. L.; Li, J. P.; Lin, C. L. *Appl. Phys. Lett.* **2004**, *84*, 3654.

(3) Lao, C. S.; Liu, J.; Gao, P. X.; Zhang, L. Y.; Davidovic, D.; Tummala, R.; Wang, Z. L. *Nano Lett.* **2006**, *6*, 263.

(4) Qian, F.; Gradecak, S.; Li, Y.; Wen, C. Y.; Lieber, C. M. *Nano Lett.* **2005**, *5*, 2287.

(5) Cui, Y.; Wei, Q. Q.; Park, H. K.; Lieber, C. M. *Science* **2001**, *293*, 1289.

(6) Huang, Y.; Duan, X. F.; Wei, Q. Q.; Lieber, C. M. *Science* **2001**, *291*, 630.

(7) Zhong, Z. H.; Qian, F.; Wang, D. L.; Lieber, C. M. *Nano Lett.* **2003**, *3*, 343.

(8) He, H.; Lao, C. S.; Chen, L. J.; Davidovic, D.; Wang, Z. L. *J. Am. Chem. Soc.* **2005**, *127*, 16376.

(9) Stern, E.; Cheng, G.; Klemic, J. F.; Broomfield, E.; Turner-Evans, D.; Li, C.; Zhou, C.; Reed, M. A. *J. Vac. Sci. Technol., B* **2006**, *24*, 231.

(10) Goldberger, J.; Sirbuly, D. J.; Law, M.; Yang, P. *J. Phys. Chem. B* **2005**, *109*, 9.

(11) Li, Y.; Wong, C. P. *Appl. Phys. Lett.* **2006**, *89*, 112112.

(12) Li, Y.; Moon, K. S.; Wong, C. P. *J. Electron. Mater.* **2005**, *34*, 266.

(13) Jiang, H. J.; Moon, K. S.; Li, Y.; Wong, C. P. *Chem. Mater.* **2006**, *18*, 2969.

(14) Duan, X. F.; Huang, Y.; Lieber, C. M. *Nano Lett.* **2002**, *2*, 487.

(15) Cui, Y.; Zhong, Z. H.; Wang, D. L.; Wang, W. U.; Lieber, C. M. *Nano Lett.* **2003**, *3*, 149.

(16) Li, C.; Fan, W. D.; Lei, B.; Zhang, D. H.; Han, S.; Tang, T.; Liu, X. L.; Liu, Z. Q.; Asano, S.; Meyyappan, M.; Han, J.; Zhou, C. W. *Appl. Phys. Lett.* **2004**, *84*, 1949.

(17) Wang, Z. L.; Song, J. H. *Science* **2006**, *312*, 242.

(18) Wang, X. D.; Zhou, J.; Song, J. H.; Liu, J.; Xu, N. S.; Wang, Z. L. *Nano Lett.* **2006**, *6*, 2768.

(19) Pan, Z. W.; Dai, Z. R.; Wang, Z. L. *Science* **2001**, *291*, 1947.

(20) Gao, P. M.; Ding, Y.; Mai, W. J.; Hughes, W. L.; Lao, C. S.; Wang, Z. L. *Science* **2005**, *309*, 1700.

(21) Lao, C. S.; Gao, P. M.; Sen Yang, R.; Zhang, Y.; Dai, Y.; Wang, Z. L. *Chem. Phys. Lett.* **2006**, *417*, 358.

(22) Huang, M. H.; Mao, S.; Feick, H.; Yan, H. Q.; Wu, Y. Y.; Kind, H.; Weber, E.; Russo, R.; Yang, P. D. *Science* **2001**, *292*, 1897.

(23) de Boer, B.; Hadipour, A.; Mandoc, M. M.; van Woudenbergh, T.; Blom, P. W. M. *Adv. Mater.* **2005**, *17*, 621.

(24) Heo, Y. W.; Tien, L. C.; Norton, D. P.; Kang, B. S.; Ren, F.; Gila, B. P.; Pearton, S. J. *Appl. Phys. Lett.* **2004**, *85*, 2002.

(25) Li, Q. H.; Wan, Q.; Liang, Y. X.; Wang, T. H. *Appl. Phys. Lett.* **2004**, *84*, 4556.

(26) Chen, J.; Reed, M. A.; Rawlett, A. M.; Tour, J. M. *Science* **1999**, *286*, 1550.

(27) Cornil, J.; Calbert, J. P.; Bredas, J. L. *J. Am. Chem. Soc.* **2001**, *123*, 1250.

(28) Donhauser, Z. J.; Mantooth, B. A.; Kelly, K. F.; Bumm, L. A.; Monnell, J. D.; Stapleton, J. J.; Price, D. W.; Rawlett, A. M.; Allara, D. L.; Tour, J. M.; Weiss, P. S. *Science* **2001**, *292*, 2303.

(29) Liu, J.; Gao, P. X.; Mai, W. J.; Lao, C. S.; Wang, Z. L. *Appl. Phys. Lett.* **2006**, *89*.

(30) Zhou, J.; Liu, J.; Yang, R. S.; Lao, C. S.; Gao, P. X.; Tummala, R.; Xu, N. S.; Wang, Z. L. *Small* **2006**, *2*, 1344.